Proc. of The Third Intl. Conf. on Advances in Computing, Control and Networking - ACCN 2015.

ISBN: 978-1-63248-082-8 doi: 10.15224/ 978-1-63248-082-8-09

Numerical Investigation of Packed-Bed Thermal Energy Storage Systems with Prediction-based Adjustment of the Heat Transfer Fluid Flow

Daniela Dejaco[1], Antonello Baccoli[1], Alessandro Pisano[1,*], Elio Usai[1], Martin Horn[2], Giorgio Cau[3], Pierpaolo Puddu[3], Fabio Serra[4]

***Abstract*—This paper numerically investigates ad-hoc charging strategies for a Packed Bed Thermal Energy Storage System. We derive a mathematical model of the system, whose reliability is assessed through comparison with experimental measurements taken on a laboratory-scale prototype with the packed bed made of alumina particles and air being used as the heat transfer media. Then we show by numerical investigations that certain non-constant flow profiles, which are determined on the basis of a predictive mechanism, yield a more effective use of the considered sensible heat storage apparatus in comparison to the commonly adopted constant-flow charging/discharging process.**

Keywords. Thermal Energy Storage System. Sensible heat storage, Packed-bed technology.

I. INTRODUCTION

Energy storage is necessary to efficiently exploit the renewable energy sources, which are inherently intermittent [1,2]. For concentrated solar power (CSP) plants in particular, storage of heat permits the uninterrupted production in the presence or absence of the solar radiation [3-7]. In [5] the main thermal energy storage (TES) technologies were surveyed, and particularly the sensible heat storage and latent heat storage solutions were compared. Sensible heat storage raises the temperature of a solid medium, whereas the latent heat storage solution includes a phase change and implies the selection of an appropriate phase change material (PCM). Sensible heat storage is currently recognized as the simplest and cheapest method to store thermal energy [8]. Sensible heat TES systems with a single tank filled with solid material (packed bed) of high thermal capacity have been proposed. A storage system with a single tank is about 35% cheaper than the system with two tanks where the storage medium is the same heat transfer fluid (HTF) [9]. In the system with a single tank, the hot and cold fluids are separated by a region, called thermocline, which is characterized by a strong gradient of temperature that mainly depends on the characteristics of the solid storage material. Systems with packed bed (refractory ceramic materials, concrete, and limestone are most often utilized due to their relatively low cost and high thermal capacity) have been widely studied. Many published works (see e.g. [8, 10-14].) refer for numerical investigations to the mathematical PDE model originally developed by Schumann [12].

The main objective of this work is to analyze the transient of the temperature distribution along the storage system and the formation of the thermocline for a loading cycle performed using suitably non-constant profiles for the flow of the HTF across the packed bed which are generated through a feedback-based control scheme. It is shown that such non-constant patterns for the HTF flow profile yield the higher percentage of loading within a given time as compared to the conventional constant-flow operation. At the same time, the non-constant flow patterns speed up the loading transient for a given desired percentage of loading as compared to the constant-flow scenario. The numerical investigation is based on a two-phase one-dimensional modified Schumann model, where all the thermodynamic properties of the fluid are temperature dependent. The mathematical model is validated by means of experimental measurements taken on a laboratory scale prototype operating at constant flow, and the mathematical model is subsequently used to perform the variable-flow loading test.

Section II illustrates the considered mathematical model, with the Subsection II.A reporting the parameter values of the laboratory-scale prototype. Section III presents the numerical investigation of the loading phase under constant and variable HTF flow conditions. Section IV draws some final conclusions and perspectives for next research.

II. MATHEMATICAL MODEL OF THE THERMAL STORAGE SYSTEM

The Storage System consists of a thermally isolated cylinder filled with the packed bed solid material with high thermal capacity. During the loading phase, the hot HTF flows through the cylinder and conveys the thermal energy to the packed bed, whereas the reversed flow of the cold HTF is applied to collect the energy from the solid material in the discharging phase.

The mathematical model to be developed is a LTNE (Local Thermal Non-Equilibrium) model based on Schumann's equations for heat transfer in a porous prism [12]. It is a two

[1] Department of Electrical and Electronic Engineering, University of Cagliari, Cagliari, Italy.
[2] Institute of Automation and Control, Technical University of Gratz, Gratz, Austria.
[3] Department of Mechanical, Chemical and Material Engineering, University of Cagliari, Cagliari, Italy.
[4] Solar Concentration Technologies and Hydrogen from RES Laboratory, Sardegna Ricerche , Cagliari, Italy
[*]Corresponding author. E-mail: pisano@diee.unica.it

Proc. of The Third Intl. Conf. on Advances in Computing, Control and Networking - ACCN 2015.

ISBN: 978-1-63248-082-8 doi: 10.15224/ 978-1-63248-082-8-09

phase 1D model consisting of two coupled PDEs which enable the calculation of the transient spatio-temporal evolution of the solid ($T_b(x,t)$) and fluid ($T_f(x,t)$) temperature under the assumptions that:

- The temperature gradient in the radial direction is zero
- The cylinder is thermally isolated
- The heat transfer rate from fluid to solid at any point is proportional to the average difference in temperature between fluid and solid at that point
- Thermal expansion can be neglected in both the fluid and the solid

The two coupled PDEs (see [12,15,16] for the derivation and further details) take the form

$$\frac{\partial T_f}{\partial t} = -\frac{\dot{m}_f C_{P,f}}{\rho_f \varepsilon C_{V,f} A}\frac{\partial T_f}{\partial x} + \frac{h_V}{\rho_f \varepsilon C_{V,f}}\left(T_b - T_f\right), \quad (1)$$

$$\frac{\partial T_b}{\partial t} = \frac{6h}{\rho_b d_S C_{V,b}}\left(T_f - T_b\right), \quad (2)$$

$$h = \frac{k_f}{d_S}\left(2 + 1.1\left(\frac{C_{P,f}\mu_f}{k_f}\right)^{1/3}\left(\frac{\dot{m}_f d_S}{A\mu_f}\right)^{0.6}\right), \quad (3)$$

$$h_V = \frac{6h(1-\varepsilon)}{d_S}, \quad (4)$$

where the meaning of the parameters is explained in the following table (the subscript *b* refers to the solid bed and the subscript *f* refers to the fluid respectively);

TABLE I. MEANING OF PARAMETERS

Parameter	Unit	Description
$\dot{m}_f$	kg/s	Massic flow of the HTF
$C_{V,f}$ / $C_{V,b}$	J/kgK	Specific heat at constant volume
$C_{P,f}$ / $C_{P,b}$	J/kgK	Specific heat at constant pressure
ε	[0,1]	Bed void fraction
ρ_f / ρ_b	kg/m^3	Density
A	m^2	Tank cross section
h	Wm^2/K	Heat transfer coefficient
d_S	m	Average diameter of the packet bed particles
k_f	W/mK	Thermal conductivity of the fluid
μ_f	Pa s	Dynamic viscosity of the fluid

A. *Physical parameters of the laboratory-size setup*

The schematics and picture of the laboratory setup are shown in the Figures I. The geometrical properties of the tank are:

L=1.8 m Height of the tank
R=0.292 m Diameter of the tank
A=π R^2=0.26 m^2 Tank cross section

The admissible air flow is limited between the minimum and maximum values

$$0.07 \text{ kg/s} \le \dot{m}_f \le 0.7 \text{ kg/s}$$

The temperatures of the hot and cold mass air flow are

T_{hot}=237 °C T_{cold}=38 °C

Air is adopted as the HTF. All thermo-physical properties of the air are assumed to be dependent on the temperature T_f (see Fig. II). Polynomial approximations of the first or second order are used to fit the temperature dependence of the thermo-physical coefficients. The material chosen for the particles is mostly composed of aluminum oxide, and its thermo-physical properties are also assumed to be dependent on the temperature T_f (see Fig. II).The average diameter of the packet bed particles is d_S=0.008 m, whereas the bed void fraction is ε=0.39.

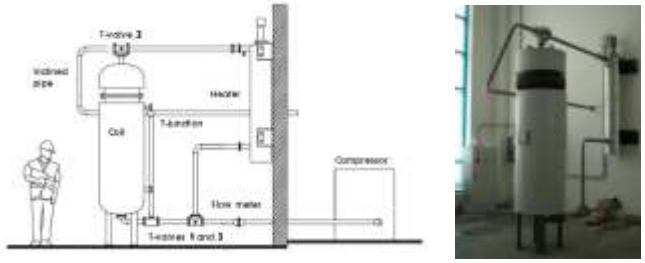

FIGURE I. LABORATORY SETUP SCHEMATICS (LEFT) AND PICTURE (RIGHT)

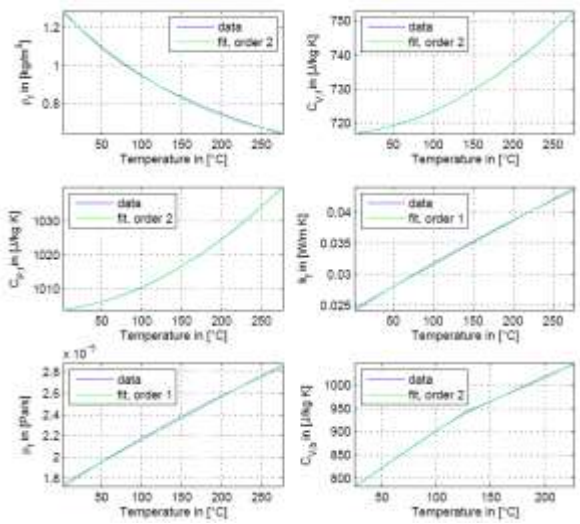

FIGURE II. THERMOPHYSICAL PROPERTIES OF AIR AND ALUMINA WITH VARYING TEMPERATURE

III. NUMERICAL INVESTIGATIONS

To solve the system (1)-(4), the Lax-Wendroff discretization method is adopted, which implements a simultaneous spatial/temporal discretization with the spatial and temporal steps

Δ*x*=0.025 m Spatial discretization
Δ*t*=0.0025 s Temporal discretization

chose in order to satisfy (for each admissible temperature and flow values) the inequality

Proc. of The Third Intl. Conf. on Advances in Computing, Control and Networking - ACCN 2015.

ISBN: 978-1-63248-082-8 doi: 10.15224/ 978-1-63248-082-8-09

$$CFL = \frac{\dot{m}_f C_{P,f}}{\rho_f \ \varepsilon \ C_{V,f} A} \frac{\Delta t}{\Delta x} < 1 \qquad (5)$$

involving the so-called Courant-Friedrichs-Lewy (CFL) number ensuring the stability of the Lax-Wendroff numerical model. The chosen spatial discretization yields $L/\Delta x=72$ spatial "nodes" where the temperatures T_f and T_b are computed by the model. The initial conditions (t=0) are

$$T_f(x,0) = T_b(x,0) = T_{cold}$$

In the experimental prototype the fluid temperature is measured by temperature sensors embedded into the tank at 19 different vertical locations equispaced within the height L of the tank. The first and last sensors measure the temperature at the top (x=0) and bottom (x=L=1.8m) side of the tank. Since the height of the tank is L=1.8m, the spacing between the thermocouples is thus 0.1m. For validating the mathematical model, a charging test was made in the laboratory system using the constant HTF mass flow $\dot{m}_f$ = 0.15 kg/s, and the temperature measurements were recorded. Figure III compares the laboratory measurements (T_{lab}) and the response of the mathematical model at the locations of the sensors (T_0, T_1, …). The maximal discrepancy exceeds 10 degrees, but the majority of the mismatches do not exceed the 5 degrees. The bigger error is exclusively found in the temperature T_6, which might be due to an incorrect positioning of the corresponding sensor. Figure IV shows the measured and simulated spatial thermocline profiles at various time instants, showing the good accuracy of the model. The model slightly overestimates the state of charge of the tank, which is due to the several losses that were neglected in the model.

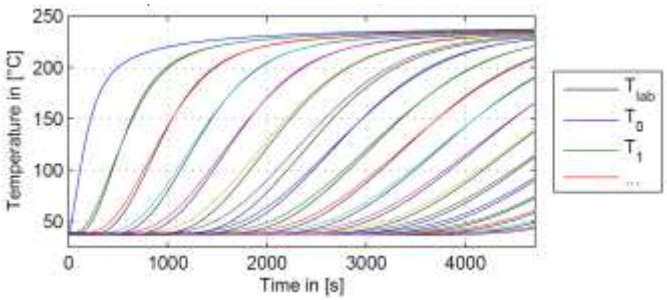

FIGURE III. MODEL VALIDATION TEST. MEASURED VS. SIMULATED TEMPERATURE PROFILES.

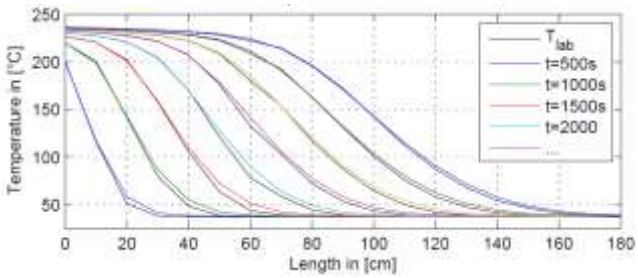

FIGURE IV. MODEL VALIDATION TEST. MEASURED VS. SIMULATED THERMOCLINE AT VARIOUS TIME INSTANTS

We will assume that the system is charged at the instant $t=t_{charged}$ at which the temperature of the fluid at the lower end of the cylinder (x=180 cm) will rise by 7.5 degrees from the initial value. Figure V displays the predicted charging time for different values of the constant mass flow between the limit values $\dot{m}_{f,MIN} = 0.07 kg/s$ and $\dot{m}_{f,MAX} = 0.26 kg/s$. It is seen that higher flows speed up the charging transient. Such predicted profile will later be used to perform the predictive adjustment strategy of the HTF flow.

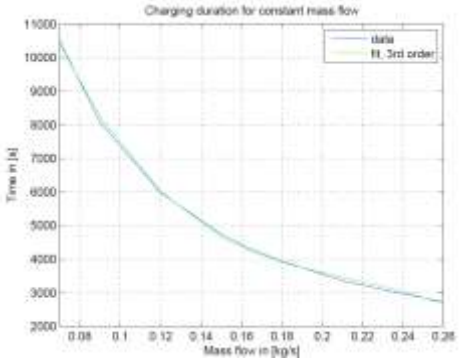

FIGURE V. CHARGING TIME WITH CONSTANT FLOW

At this point one could inadvertently conclude that the charging with higher mass flow is always is in general favorable. Figure VI depicts the corresponding **percentage of charge** PoC computed through the formula

$$PoC = \frac{\int_0^L \{T_b(x, t_{charged}) - T_{cold}\} dx}{L(T_{hot} - T_{cold})} \times 100$$

Figure VI shows that the price to be paid to speed up the charging transient with constant flow is the lowering of the percentage of charge.

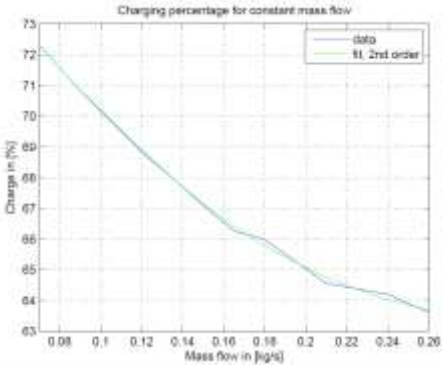

FIGURE VI. PERCENTAGE OF CHARGE WITH CONSTANT FLOW

Different flow profiles were tested to investigate the possibility of improving the performance compared to the constant-flow charging test. Such non-costant profiles are shown in the Figure VII. The profiles n. 1 and 2 are built according to pre-specified patterns commuting between the maximal and minimal flows $\dot{m}_{f,MIN}$ and $\dot{m}_{f,MAX}$. Particularly, the switch is started in the profile n.1 at the time instant t_{s1} given by

Proc. of The Third Intl. Conf. on Advances in Computing, Control and Networking - ACCN 2015.

ISBN: 978-1-63248-082-8 doi: 10.15224/ 978-1-63248-082-8-09

$$t_{s1} = \frac{1}{2} t_c\left(\dot{m}_{f,MAX}\right)$$

where the predicted charging time function $t_c(.)$ is displayed in the Figure V. Similarly, the switch is started in the profile n.2 at the time instant t_{s2} given by

$$t_{s2} = \frac{1}{2} t_c\left(\dot{m}_{f,MIN}\right)$$

The profile n.3, on the contrary, features a ramp-shaped HTF flow profile joining the limit values $\dot{m}_{f,MIN}$ and $\dot{m}_{f,MAX}$ where the activation time instant of the ramp is a-priori set to t_{a3}=100s. Thus the profiles n. 1 and 2 are prediction based, whereas the profile n. 3 is determined in open loop.

The profiles n. 2 and 3 are expected to give the best performance. In fact, at the beginning of the charging process the difference between the fluid and solid temperatures is small and the heat exchange is consequently weak. A lower flow can provide a more efficient heat exchange in the initial part of the charging process. The flow can subsequently be increased when the difference between the fluid and solid temperatures has raised and good heat exchange can be achieved also at high flows. Table II reports the charging times and PoC obtained using different constant values of the flow (upper part of the table) and the results achieved using the three noncostant profile. It is seen, for instance, that the experiment 2 provides nearly the same PoC than with the constant flow $\dot{m}_f$ = 0.09 kg/s but with the shorter charging time (6579 s. against 8069 s). Figure VIII

This performance improvement is captured by the plot of Figure VIII, the two variable-flow experiments staying above the solid curve being those providing the better performance than the constant-flow ones.

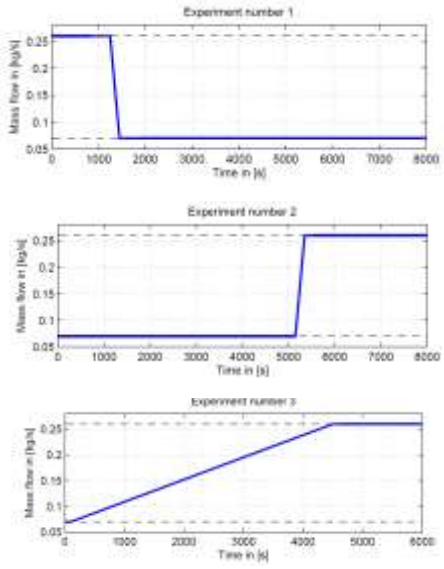

FIGURE VII. NON-CONSTANT HTF FLOW PROFILES

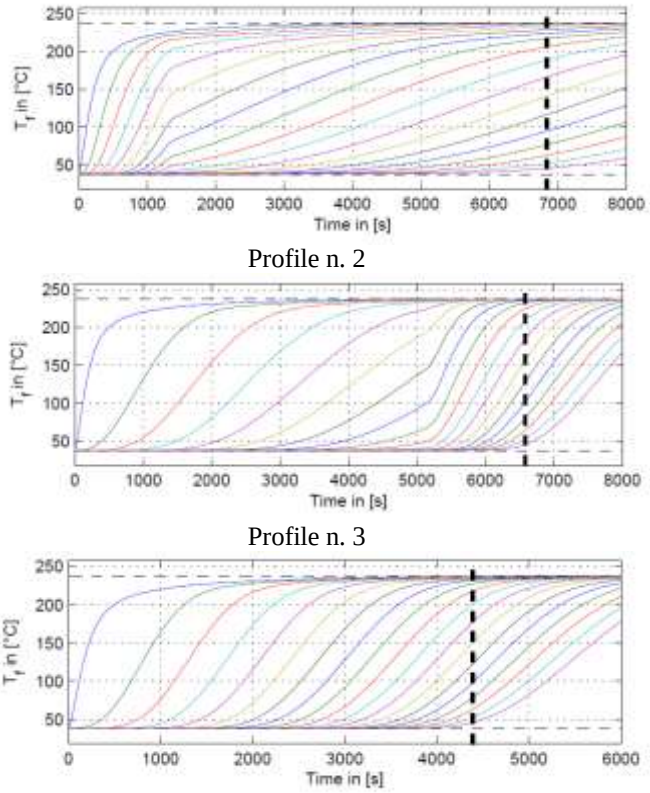

FIGURE VIII. TEMPORAL EVOLUTIONS OF THE FLUID TEMPERATURES AT THE MEASUREMENT NODES WITH THE NONCOSTANT HTF LOW PROFILES

TABLE II CONSTANT VS. VARIABLE FLOW CHARGING PERFORMANCE

	$t_{charged}$ in [s]	$\%_{charged}$
$\dot{m}_f = 0.07 kg/s$	10482	72.3
$\dot{m}_f = 0.09 kg/s$	8069	70.83
$\dot{m}_f = 0.12 kg/s$	5978	68.87
$\dot{m}_f = 0.15 kg/s$	4735	67.1
$\dot{m}_f = 0.165 kg/s$	4286	66.27
$\dot{m}_f = 0.18 kg/s$	3943	65.98
$\dot{m}_f = 0.21 kg/s$	3359	64.56
$\dot{m}_f = 0.24 kg/s$	2966	64.2
$\dot{m}_f = 0.26 kg/s$	2727	63.61
Experiment 1	6840	66.69
Experiment 2	6579	70.19
Experiment 3	4390	68.5

IV. CONCLUSIONS

With reference to the packed-bed heat storage apparatus, it has been shown by numerical investigations that non constant flow profiles can improve the charging performance compared to the constant-flow scenario. Besides making variable-flow experiments, which was not possible with the current experimental setup, more in depth investigations devoted to optimally design the variable flow profiles will be the subject of next research. Repeated charging/discharging phases will be studied to further improve the robustness and performance. More powerful predictive strategies incorporating model-based optimization algorithms such as the Model Predictive Control

Proc. of The Third Intl. Conf. on Advances in Computing, Control and Networking - ACCN 2015.

ISBN: 978-1-63248-082-8 doi: 10.15224/ 978-1-63248-082-8-09

appear to be a particularly promising class of approaches to be considered for future research within the present framework.

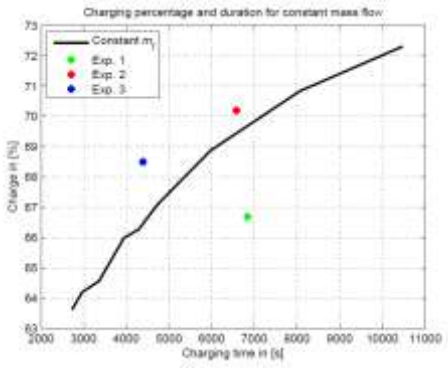

FIGURE IX. CHARGING TIME VS. POC WITH CONSTANT AND VARYING FLOWS

ACKNOWLEDGMENTS

The research leading to these results has received funding from the research project “Modeling, control and experimentation of innovative thermal storage systems”, funded by Sardinia regional government under grant agreement n. CRP-60193

REFERENCES

[1] P. Li Energy storage is the core of renewable energy technologies. IEEE Nanotechnol Mag 2008;4:3–18.

[2] G.J. Kolb Economic evaluation of solar-only and hybrid power towers using molten-salt technology. Sol Energy vol. 62, pp. 51–61, 1998.

[3] US Department of Energy, SunShot vision study, February 2012. p. 115 [chapter 5].

[4] Schmidt FW, Willmott AJ. Thermal energy storage and regeneration. Washington, DC: Hemisphere Pub. Corp; 1981.

[5] S.M. Hasnain “Review on sustainable thermal energy storage technologies, Part I: heat storage materials and techniques”. Energy Convers Manag; vol. 39, :pp. 1127–1138, 1998

[6] U. Herrmann, DW Kearney Survey of thermal energy storage for parabolic trough power plants. ASME Trans J Sol Energy Eng, vol. 124, pp. 145–52, 2002.

[7] Zalba B, Marin JM, Cabeza LF, Mehling H. Review on thermal energy storage with phase change: materials, heat transfer analysis and applications. Appl Therm Eng 2003;23:251–83

[8] A. Gil et al., State of the art on high temperature thermal energy storage for power generation. Part 1—Concepts, materials and modellization, Renewable and Sustainable Energy Reviews 14 (2010) 31–55.

[9] Brosseau D, Kelton JW, Ray D, Edgar M, Chisman K, Emms B. Testing of thermocline filler materials and molten-salt heat transfer fluids for thermal energy storage systems in parabolic trough power plants. J Solar Energy Eng-Trans ASME 2005;127:109–16.

[10] J. Coutier, E. Farber, Two applications of a numerical approach of heat-transfer process within rock beds, Sol. Energy 29 (6) pp. 451-462, 1982.

[11] G. Adebiyi, E. Nsofor, W. Steele, A. Jalalzadeh-Azar, Parametric study on the operating efficiencies of a packed bed for high-temperature sensible heat storage, ASME J. Sol. Energ. Eng. 120 (1) (1998) 2-13.

[12] T. Schumann, Heat transfer: a liquid flowing through a porous prism, J. Franklin Inst. 208 (1929) 405-416.

[13] K. Ismail, R. Stuginsky, A parametric study on possible fixed bed models for pcm and sensible heat storage, Appl. Therm. Eng. 19 (7) (1999) 757-788.

[14] Harmeet Singh, R.P. Saini, J.S. Saini, A review on packed bed solar energy storage systems, Renewable and Sustainable Energy Reviews, vol. 14, n. 3, pp. 1059–1069, 2010

[15] K. Ismail, R. Stuginsky, A parametric study on possible fixed bed models for pcm and sensible heat storage, Appl. Therm. Eng., vol. 19, n. 7, pp. 757-788, 1999.

[16] M. Cascetta, G. Cau, P. Puddu, F. Serra, Numerical investigation of a packed bed thermal energy storage system with different heat transfer fluids, Energy Procedia, vol. 45, pp. 598 – 607, 2014.